A Theoretical Framework on Real-Time Communication and Information Estimation in Ultra Large-Scale 6G C-V2X Networks

He Huang, *Member, IEEE,* Zilong Liu*, *Senior Member, IEEE,* Haishi Wang*, *Member, IEEE,* Wei Huang, *Senior Member, IEEE,* Chaojie Gu, *Member, IEEE,* Zhiheng Hu, Md. Noor-A-Rahim, *Senior Member, IEEE,*

***Abstract*—The emergence of sixth generation communication (6G) wireless networks is set to revolutionize vehicular communication by enabling ultra-reliable, low-latency, and high-capacity connectivity in cellular vehicle-to-everything (C-V2X) environments. This paper presents a theoretical framework on novel cooperative vehicular communication and information perception algorithms for large-scale 6G C-V2X networks while leveraging integrated space-air-ground communication system. Specifically, we address key challenges in real-time information exchange and fusion among multiple vehicles. Utilizing inequality theory and functional mapping theory, we derive an upper bound on channel capacity for a fixed number of relays and propose a low-complexity, multi-class relay selection algorithm. Furthermore, we introduce an optimal mobile edge computing (MEC) based correspondence strategy to improve vehicle-to-vehicle communication, alongside an efficient information estimation algorithm to facilitate real-time data sharing. Our simulation results confirm that the proposed algorithms significantly outperform existing cooperative vehicular schemes in terms of channel capacity, while the developed evaluation theory ensures accurate cooperative perception with reduced computational complexity. The proposed framework and theoretical contributions offer a foundational basis for 6G C-V2X networks.**

***Index Terms*—6G C-V2X, ultra large scale network, upper bound of channel capacity, information estimation.**

This work was supported in part by Open Research Project of the State Key Laboratory of Industrial Control Technology, China (Grant No. ICT2026B68), Fundamental Research Funds for the Central Universities of China (Grant No. PA2024GDSK0114), Sichuan Science and Technology Program (Grant No. 2025HJRC0023), Key Laboratory of Industrial Internet of Things and Networked Control, Ministry of Education of China (Grant No. FF202503), and Major Science and Technology Projects of Sichuan Province (Grant No. 2023ZDZX0013). The work of Md Noor-A-Rahim emanated from research conducted with the financial support of Taighde Éireann – Research Ireland (Grant No. 24/FFP-P/12832). An earlier version of this paper was presented in part at the 2025 IEEE 102nd Vehicular Technology Conference (VTC2025-Fall) [DOI: 10.1109/VTC2025-Fall65116.2025.11310637.]. (Corresponding authors: Zilong Liu; Haishi Wang)

He Huang, Haishi Wang and Zhiheng Hu are with College of Communication Engineering (College of Microelectronics), Chengdu University of Information Technology, Chengdu 610225, China. He Huang is also with Intelligent Interconnected Systems Laboratory of Anhui Province, Hefei University of Technology, Hefei 230009, China, e-mail: (huanghe@cuit.edu.cn; whs@cuit.edu.cn; hzh@cuit.edu.cn)

Zilong Liu is with the School of Computer Science and Electronic Engineering, University of Essex, 1NW.4.12, Colchester Campus, UK (e-mail: zilong.liu@essex.ac.uk)

Wei Huang is with School of Computer Science and Information Engineering, also with Intelligent Interconnected Systems Laboratory of Anhui Province, Hefei University of Technology, Hefei 230009, China, e-mail: (huangwei@hfut.edu.cn)

Chaojie Gu is with College of Control Science and Engineering, Zhejiang University, Hangzhou 310027, China, e-mail: (gucj@zju.edu.cn)

Md. Noor-A-Rahim is with the nasc Research, School of Computer Science & IT, University College Cork, Cork T12 XF62, Ireland, e-mail: (m.rahim@cs.ucc.ie)

I. Introduction

THE rapid advancement of wireless communication technologies has accelerated the global commercialization and deployment of fifth generation communication (5G) networks, with infrastructures now reaching mature stages in several countries, including China [1], [2]. In parallel, research on sixth-generation (6G) wireless systems has gained significant momentum, aiming to deliver transformative improvements in communication quality, service flexibility, and the seamless integration of space-air-ground networks [3], [4]. Compared to 5G, 6G is anticipated to substantially enhance channel capacity, reduce outage probabilities (OP), improve security, and expand coverage. Furthermore, 6G will fully embrace intelligent, adaptive, and ubiquitous computing capabilities to meet the growing demands of ultra-dense internet of things (IoT) ecosystems [5], [6]. Future 6G networks are expected to integrate a wide range of foundational technologies, including free space optical (FSO) communication, integrated sensing and communication (ISAC), space-air-ground convergence, edge computing, and Artificial Intelligence (AI) [6]–[9].

Among various application scenarios envisioned for 6G, the cooperative internet of vehicles (CIoV) has emerged as particularly critical. This scenario entails extensive communication among highly dynamic vehicles and incorporates advanced technologies such as MEC, AI, and comprehensive space-air-ground integration [8], [10], [11]. Numerous research efforts have been dedicated to large-scale vehicular communication, focusing on challenges such as cooperative relay selection, AI-driven task execution across multiple vehicles, and intelligent edge computing algorithms. For instance, the development of MEC in connected vehicles has been reviewed within the context of intelligent transportation systems, where edge cloud infrastructures are proposed to enable enhanced service delivery [12]. The authors in [13] propose a tunnel-less multi-cluster overlay scheme designed to surpass existing software-defined networking mechanisms for MEC. A distributed cooperative caching and content sharing strategy is presented in [14] to maximize device-to-device (D2D) cellular traffic among neighboring devices in 5G edge networks. Under constraints on the total queue lengths of communication and computation tasks, [15] introduces an energy allocation algorithm aimed at minimizing the long-term average energy consumption within

a stochastic framework. Similarly, the authors in [16] propose a cross-layer framework that simultaneously optimizes user association, packet offloading rates, and bandwidth allocation in MEC systems. The study in [17] highlights how smart grids can benefit from 5G-based distributed state estimation schemes and provides a review of emerging state estimation techniques in 5G mobile cellular networks. Collectively, these contributions demonstrate that relays selection, resource allocation, and optimal sensing and communication are fundamental challenges that must be addressed in future ultra-large-scale C-V2X mobile networks under 6G.

On the other hand, cooperative multi-vehicle MEC networks have also emerged as significant research topics in several recent frontier studies. For example, [18] introduces a collaborative game-theoretic method to address the computation offloading problem in non-orthogonal multiple access (NOMA) enabled multi-access edge computing systems. Compared with existing schemes, the proposed algorithm demonstrates advantages in reducing computation overhead, increasing offloading efficiency, and minimizing the number of switch operations. The authors in [19] propose a layered mobile relays selection algorithm for cooperative MEC within space-air-ground integrated scenarios, achieving an optimal upper bound for channel capacity through full duplex (FD) NOMA based D2D communication. To enhance the average resource hit rate and reduce decision delay, an AI-driven cooperative resource allocation algorithm is presented for 6G massive IoT networks in [20]. Furthermore, to boost user throughput at the edge of cellular networks, [21] investigates cooperative multi-point operation techniques that improve the service quality in dense small-scale network deployments. In pursuit of greater prediction accuracy, [22] proposes an edge intelligence-based resource allocation framework for vehicular MEC networks, which also offers lower deployment costs. Overall, enabling joint multi-vehicle communication with multiple relays and MEC nodes presents a critical challenge in the realization of future 6G C-V2X networks.

A. Motivations

Against the above background, several critical challenges remain unresolved in ultra-massive C-V2X communication scenarios:

1) **Integration of Sensing Information from Vehicles:** In the 6G C-V2X era, vehicles exhibit high mobility and sense around information in real time, in order to access real-time road conditions, it is crucial to efficiently integrate sensing information of multiple vehicles together and this integration is vital for supporting future autonomous driving systems.
2) **Optimal Communication Scheme of D2D Based on Multiple Relays:** Based on **Motivation 1)**, how do we send integrated sensing information effectively? Traditional fixed base station deployments are insufficient to support reliable vehicular communication in environments characterized by high mobility. The rapid movement of vehicles often leads to coverage gaps and unstable transmission quality. Therefore, unlike [8]-[14], novel adaptive multiple relays selection mechanisms are essential to maintain robust and continuous connectivity among fast-moving vehicles.
3) **Real-Time Information Dissemination and Fusion:** Current vehicular traffic information systems rely heavily on satellite-based services (e.g., Google Maps, Baidu Maps), which often fail to reflect real-time road and traffic conditions. While standards such as IEEE 1609.X, IEEE 802.11p, and ETSI ITS-G5 exist, real-time vehicular message dissemination remains underdeveloped. This necessitates the development of new data processing frameworks capable of enabling immediate responses to dynamic traffic events in different time-slots.

B. Contributions

Addressing the challenges outlined above, this paper presents real-time sense and communication framework in Fig. 2, the primary contributions are as follows:

1) Firstly, we propose a dynamic and ultra-scalable C-V2X network topology that utilizes cooperative relays consisting of vehicles, UAVs and other mobile IoT nodes. Unlike [8]-[15], we consider that a vehicle-to-vehicle network (Fig. 2) for combining multiple vehicular functions to meet stringent 6G requirements such as higher channel capacity, ultra-low latency and low-complexity radar point cloud information fusion.
2) Secondly, in order to achieve optimal real-time communication, we prove that the channel capacity can approach to an upper bound when the number of relays is fixed. By employing inequality theory, we develop a low-complexity multi-relay selection algorithm. Compared with classical relays selection algorithms in [8], [9], [12]-[14], simulation results indicate that the proposed method yields a notable enhancement in channel capacity—approximately 0.8 *Kbps* to 2.5 *Kbps* higher than other algorithms.
3) Thirdly, according to optimal MECs subset selection algorithm, we introduce a caching mechanism that selects high-quality MEC nodes (which has not been presented in other references before) to assist with D2D data buffering and transmission. We also obtain maximum channel capacity between fast-moving vehicles with the aid of MEC-aided real-time communication paths. In addition, it is shown that the proposed algorithms support real-time communication and enhance information caching via MEC excellence selection across vehicle groups.
4) Finally, numerical results demonstrate that the proposed 6G C-V2X framework and algorithms offer significantly higher D2D channel capacity than traditional schemes. Furthermore, the proposed methods achieve better sensing information fusion and exhibit orders of magnitude improvement in computational complexity.

***Notations*:** We list main notations in **Table I**.

II. Proposed C-V2X System Model

Before we start, it is noted that all the major notations are listed in **Table I**. In Fig. 1, we consider a 6G ultra-massive

TABLE I
SUMMARY OF MAIN NOTATIONS

$\Re^{m\times n}$	Space of $m \times n$-dimensional real matrices
$\mathbf{K^T}$	Transpose of matrix $\mathbf{K}$
$\circ$	Hadamard (element-wise) product
$\lvert . \rvert$	Absolute value
$\bigcap$	Subsets intersection
$\bigcup$	Subsets union
$A \subseteq B$	Subset A belong to subset B
$\sum$	Summation
$\propto$	Positive correlation
$\in$	Belong to
$\equiv$	Modulus operation
$\forall$	For any
$i!$	Factorial of positive integer i
N^*	Non-negative integer
$A \rightarrow B$	A transmits signals to device B
$A \leftrightarrow B$	A and B transmit signals to each other
$A \rightarrow R_m \rightarrow B$	A transmits signals to B with relay R_m
$\{V_{sou}\}$	k_1 vehicles in the source set
$\{V'_{des}\}$	k_2 vehicles in the destination set
$\{R_L\}$	Relays subset with L relays
v_{k_i}	k_i-th vehicle in $\{V_{sou}\}$
v'_{k_j}	k_j-th vehicle in $\{V'_{des}\}$
R_m	m-th relay in $\{R_L\}$
Q_A	Transmission power of A
Q_{R_m}	Transmission power of relay R_m
$\{Q_{R_L}\}$	Transmission power subset of relays $\{R_L\}$
Q_{tot}	Total power of relays subset $\{R_L\}$
$y_{v'_{k_j}}$	Sensing information of vehicle v'_{k_j}
h_{AB}	Channel coefficient between A and B
σ_A^2	Variance of AWGN for A
$\mathbf{y_{A\rightarrow B}}$	Signals that A transmits to B
$\mathbf{y_{A\rightarrow B}^{R_m}}$	Signals that A transmits to B with relay R_m
$\mathbf{y_{A\rightarrow B}^{\{R_L\}}}$	Signals that A transmits to B with relays $\{R_L\}$
$SNR_{A\rightarrow B}$	SNR between A and B
$SNR_{A\rightarrow B}^{R_m}$	SNR between A and B with relay R_m
$SNR_{A\rightarrow B}^{\{R_L\}}$	SNR between A and B with relays $\{R_L\}$
$C_{v'_{k_j}\rightarrow v_{k_i}}^{R_m}$	Channel capacity for $v'_{k_j} \rightarrow R_m \rightarrow v_{k_i}$
$C_{v'_{k_j}\rightarrow v_{k_i}}^{\{R_L\}}$	Channel capacity for $v'_{k_j} \rightarrow \{R_L\} \rightarrow v_{k_i}$
M_i	The i-th MEC equipment
$\{M_q\}$	MEC subset with q MEC equipments
$\{V_{M_i}\}$	Vehicles subset that communicate with M_i
$M_i \leftrightarrow \{V_{M_i}\}$	M_i communicates with $\{V_{M_i}\}$
$\left\{R_{L_{k_2}}^{v'_{k_2}}\right\}$	L_{k_2} relays for $v'_{k_2} \rightarrow \left\{R_{L_{k_2}}\right\} \rightarrow v_{k_i}$
τ	Transmission delay
$\tau_{\{V'_{des}\}\rightarrow v_{k_i}}$	Transmission delay for $\{V'_{des}\} \rightarrow v_{k_i}$
MEC_A	MEC equipment which A communicates with
$\mathrm{Inf}_{v'_{k_j}}$	Information of v_{k_i} from v'_{k_j}
$\mathrm{Inf}_{\{V'_{des}\}}$	Information of v_{k_i} from $\{V'_{des}\}$
$\mathrm{Inf}_{\left\{V'_{subi-N_i}\right\}}$	Information of v_{k_i} from $\left\{V'_{subi-N_i}\right\}$
W	Unit: watt
$\equiv$	Modulus operation
$Kbps$	Unit: thousand bit per second
m_{R_k}	Number of factors for relay R_k
Km/h	Unit: thousand meters per hour
m	Unit: meter
$n!$	n factorial
$C_{k_2}^i$	$(k_2!)/(i!(k_2-i)!)$
NETs	Number of evaluation times

air-space-ground C-V2X ubiquitous network consisting of a large number of vehicles, unmanned aerial vehicles (UAVs), fixed base stations, and mobile edge computing (MEC). Our objective is to achieve relay aided optimal communication and efficient information estimation in cooperative C-V2X networks. Besides, we mainly assume that selected relays are sufficiently robust and are allowed to forward information to vehicles in source and destination. Following [5] and [10], it is assumed that two-hop decode-to-forward (DF) relay mode is adopted and each communication device operates in half-duplex mode with a single antenna, and we neglect the impact of multiple antennas and the resulting distinct channels for different D2D links.

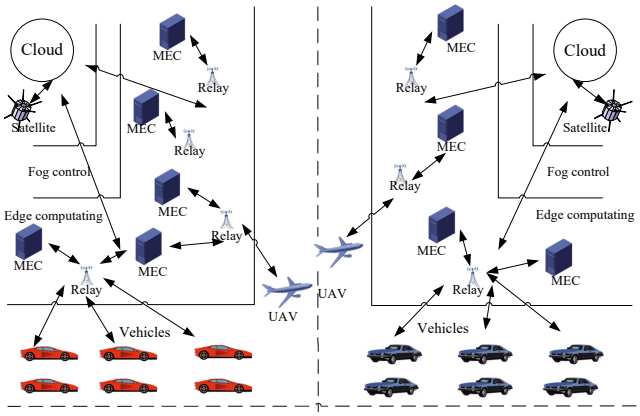

Fig. 1. 6G ultra massive C-V2X ubiquitous networks

We assume that there are $k_1(k_1 \in \mathrm{N}^*)$ mobile vehicles in the source set $\{V_{sou}\}$ and $k_2(k_2 \in \mathrm{N}^*)$ mobile vehicles in the destination set $\{V'_{des}\}$. In successive time-slots, vehicles in $\{V'_{des}\}$ firstly sense around for the real-time traffic conditions and channel state information, before selecting certain relay subsets, such as vehicle relays, UAV relays, mobile relays (e.g., handsets, laptops, and small IoT devices), base station relays, and MEC devices. Afterwards, the vehicles in $\{V'_{des}\}$ send back the sensed environmental information to cooperative relays and MEC devices, whereby the latter cache and compute those sensing data from $\{V'_{des}\}$. Finally, relays and MEC devices transmit these sensing data to $\{V_{sou}\}$. Hence, in the presented dynamic C-V2X mobile networks, as vehicles keep moving, both the power allocation and channel fading coefficients may change. More information on this can be found in **Section VI. A, B**, (42) and (43). (Moveover, such a dynamic analysis method has also been applied in [9-14]).

It is assumed that the vehicles in $\{V_{sou}\}$ and $\{V'_{des}\}$ are distinct from the vehicles in the cooperative relays. In the subsequent sections, we first investigate optimal communication algorithm with relays (**Section III**) and MECs (**Section IV**), then we investigate effective information estimation for multiple vehicles (**Section V**).

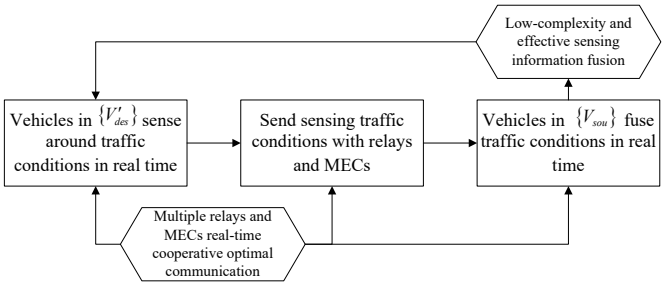

Fig. 2. Real-time sense and communication process for multiple ultra large-scale device subsets

III. Optimal communication in ultra-large-scale C-V2X networks

A. D2D communication for single vehicle to single vehicle

Considering the communication process presented in **Section II**, we assume that for a source set $\{V_{sou}\}$ with k_1 vehicles and a destination set $\{V'_{des}\}$ with k_2 vehicles, let $\forall v_{k_i}$ be a vehicle in $\{V_{sou}\}$ (defined as $\{V_{sou}\} = (v_1, v_2, ..., v_{k_1})$) where $1 \leq k_i \leq k_1$, and $\forall {v'}_{k_j}$ be a vehicle in $\{V'_{des}\}$, defined as $\{V'_{des}\} = ({v'}_1, {v'}_2, ..., {v'}_{k_2})$, where $1 \leq k_j \leq k_2$. When ${v'}_{k_j}$ sends signals to v_{k_i} (${v'}_{k_j} \rightarrow v_{k_i}$), an arbitrary set of L relays (defined as $\{R_L\} = (R_1, R_2, \ldots, R_L)$, where $L \in \mathrm{N}^*$) is selected from the total relay set.

Furthermore, we assume the transmission power of relay R_m is Q_{R_m} for $R_m \in \{R_L\}$, and the transmission powers of the relay subset $\{R_L\}$ are given by $\{Q_{R_L}\} = (Q_{R_1}, Q_{R_2}, \ldots, Q_{R_L})$. In certain time-slot, the sensing information of vehicle ${v'}_{k_j}$ is $y_{{v'}_{k_j}}$, its transmission power is $Q_{{v'}_{k_j}}$, the channel coefficient between ${v'}_{k_j}$ and relay R_m is $h_{{v'}_{k_j}R_m}$, and the noise at relay R_m is modeled as additive white Gaussian noise (AWGN) with variance $\sigma^2_{R_m}$. We assume the following dimensions for the vectors: $\mathbf{y_{v'_{k_j} \rightarrow R_m}} \in \Re^{1\times n}$, $\mathbf{v'_{k_j}} \in \Re^{1\times n}$, $\mathbf{R_m} \in \Re^{1\times n}$, $\mathbf{Q_{v'_{k_j}}} \in \Re^{1\times n}$, $\mathbf{h_{v'_{k_j}R_m}} \in \Re^{1\times n}$, $\mathbf{y_{v'_{k_j}}} \in \Re^{1\times n}$, and $\boldsymbol{\sigma^2_{R_m}} \in \Re^{1\times n}$. In the first time-slot, the signal which relay $\mathbf{R_m}$ received from vehicle $\mathbf{v'_{k_j}}$ is expressed as:

$$\mathbf{y_{v'_{k_j} \rightarrow R_m}} = \sqrt{\mathbf{Q_{v'_{k_j}}}} \circ \mathbf{h_{v'_{k_j}R_m}} \circ \mathbf{y_{v'_{k_j}}} + \boldsymbol{\sigma^2_{R_m}}. \quad (1)$$

Supposing that the channel coefficients of $\mathbf{R_m} \rightarrow \mathbf{v_{k_i}}$ is $\mathbf{h_{R_m v_{k_i}}}$, and the noise at $\mathbf{v_{k_i}}$ is AWGN with variance $\boldsymbol{\sigma^2_{v_{k_i}}}$. Depending on DF relays, the received signal in the second time-slot is given by

$$\mathbf{y_{R_m \rightarrow v_{k_i}}} = \sqrt{\mathbf{Q_{R_m}}} \circ \mathbf{h_{R_m v_{k_i}}} \circ \mathbf{y_{v'_{k_j} \rightarrow R_m}} + \boldsymbol{\sigma^2_{v_{k_i}}}. \quad (2)$$

Substituting (1) into (2), the signal received by $\mathbf{v_{k_i}}$ from $\mathbf{v'_{k_j}}$ through relay $\mathbf{R_m}$ is obtained as $\mathbf{y^{R_m}_{v'_{k_j} \rightarrow v_{k_i}}}$. When the selected relay subset is $\{R_L\}$, the combined received signal is denoted as $\mathbf{y^{\{R_L\}}_{v'_{k_j} \rightarrow v_{k_i}}}$. The corresponding SNR for the transmission from $\mathbf{v'_{k_j}}$ to $\mathbf{v_{k_i}}$ via the relay set $\{R_L\}$ is given by (3), as shown at the top of the next page.

Lemma 1 Upper bound of SNR for single vehicle to single vehicle: Consider L distinct communication paths from vehicle v'_{k_j} to vehicle v_{k_i} via relays $R_1, R_2, \ldots, R_L$, respectively. If the noise variance at v_{k_i} is zero, i.e., $\sigma^2_{v_{k_i}} = 0$, then SNR for the combined path $SNR^{\{R_L\}}_{v'_{k_j} \rightarrow v_{k_i}}$ is upper-bounded by the sum of the SNRs for the individual paths $\sum_{w=1}^{L} SNR^{R_w}_{v'_{k_j} \rightarrow v_{k_i}}$.

Proof: Please refer to Appendix A.

In this paper, focusing on the theoretical benchmark aspect, we have adopted a simplified system model by assuming that a robust and resilient V2X physical layer will deal with research issues caused by mobility.

It is noteworthy that in **Lemma 1**, when $\sigma^2_{v_{k_i}} \neq 0$, one can obtain an upper bound of D2D SNR in practical scenes. In fact, with the aid of (50), (51) and (60), we have (4). In (4), although we may not directly obtain the optimal upper bound, by means of optimal relay diversity selection and efficient power allocation (**Section III**, **part B**), we can attain an SNR value which is close to the theoretical upper bound value. On the other hand, $\sigma^2_{v_{k_i}}$ is irrelevant to some other key factors (e.g., power values, channel coefficients, and relay diversity).

Therefore, based on **Lemma 1**, we conclude that in real cooperative D2D communication, adjusting the transmission strategy of each relay to maximize the D2D SNR yields near-optimal SNR, thereby enhancing communication quality. Furthermore, we evaluate the maximum upper bounds for $SNR^{\{R_L\}}_{v'_{k_j} \rightarrow v_{k_i}}$ and $\sum_{w=1}^{L} SNR^{R_w}_{v'_{k_j} \rightarrow v_{k_i}}$, revealing potential optimal channel capacity bounds in 6G cooperative multi-path ultra-massive mobile networks. Additionally, we determine the upper bound of optimal communication when two arbitrary mobile devices are located in specific positions. Moreover, an optimal cooperative strategy can be identified to optimize D2D communication for any two fixed devices in 6G intelligent Internet of Everything (IoE) networks.

Lemma 2 Derivation of the SNR upper bound for ${v'}_{k_j} \rightarrow \{R_L\} \rightarrow v_{k_i}$: In view of **Lemma 1**, we derive upper bound of $SNR^{\{R_L\}}_{v'_{k_j} \rightarrow v_{k_i}}$. For relay R_t, we define:

$$\begin{cases} \varphi_1(R_t) = \sqrt{Q_{R_t}} h_{R_t v_{k_i}} \sqrt{Q_{{v'}_{k_j}}} h_{{v'}_{k_j} R_t} y_{{v'}_{k_j}} \\ \varphi_2(R_t) = \sqrt{Q_{R_t}} h_{R_t v_{k_i}} \sigma^2_{R_t}. \end{cases} \quad (5)$$

We assume that $\{R_L\}$ is

$$R_{g*} \cup (R'_1, R'_2, ..., R'_{L-1}). \quad (6)$$

On one hand, if $\forall R_t \in \{R_L\}$ and $\sigma^2_{R_t} \neq 0$, the functions of $\varphi_1(\cdot)$ and $\varphi_2(\cdot)$ are constrained by:

$$\frac{\varphi_1(R_{g*})}{\varphi_2(R_{g*})} \geq \frac{\varphi_1(R'_1)}{\varphi_2(R'_1)} \geq \frac{\varphi_1(R'_2)}{\varphi_2(R'_2)} \geq ... \geq \frac{\varphi_1(R'_{L-1})}{\varphi_2(R'_{L-1})}. \quad (7)$$

If $L = N$, the upper bound of optimal D2D SNR for multi-path cooperative communication ${v'}_{k_j} \rightarrow v_{k_i}$ with relay subset $\{R_L\}$ is given by

$$\frac{(\varphi_1(R_{g*}))^2}{(\varphi_2(R_{g*}))^2 + (\sigma^2_{v_{k_i}})^2}. \quad (8)$$

$$SNR^{\{\mathbf{R_L}\}}_{\mathbf{v'_{k_j}}\to\mathbf{v_{k_i}}}=\frac{\left|\sqrt{\mathbf{Q_{\{R_L\}}}}\circ\mathbf{h_{\{R_L\}v_{k_i}}}\circ\sqrt{\mathbf{Q_{v'_{k_j}}}}\circ\mathbf{h_{v'_{k_j}\{R_L\}}}\right|^{\mathbf{2}}}{\left|\sqrt{\mathbf{Q_{\{R_L\}}}}\circ\mathbf{h_{\{R_L\}v_{k_i}}}\circ\boldsymbol{\sigma}^{\mathbf{2}}_{\mathbf{\{R_L\}}}\right|^{\mathbf{2}}+\left|\boldsymbol{\sigma}^{\mathbf{2}}_{\mathbf{v_{k_i}}}\right|^{\mathbf{2}}}\circ\left|\mathbf{y_{v'_{k_j}}}\right|^{\mathbf{2}}. \tag{3}$$

$$\frac{\left(\sum\limits_{g=1}^{L}\sqrt{Q_{R_g}}h_{R_gv_{k_i}}\sqrt{Q_{v'_{k_j}}}h_{v'_{k_j}R_g}y_{v'_{k_j}}\right)^2}{\left(\sum\limits_{g=1}^{L}\sqrt{Q_{R_g}}h_{R_gv_{k_i}}\sigma_{R_g}\right)^2+\left(L\sigma^2_{v_{k_i}}\right)^2}\le\frac{\left(\sum\limits_{g=1}^{L}\sqrt{Q_{R_g}}h_{R_gv_{k_i}}\sqrt{Q_{v'_{k_j}}}h_{v'_{k_j}R_g}y_{v'_{k_j}}\right)^2}{\left(\sum\limits_{g=1}^{L}\sqrt{Q_{R_g}}h_{R_gv_{k_i}}\sigma_{R_g}\right)^2}\le\sum_{w=1}^{L}SNR^{R_w}_{v'_{k_j}\to v_{k_i}}|(\sigma^2_{v_{k_i}}=0). \tag{4}$$

On the other hand, for $(R'_1,R'_2,...,R'_{L-1})$, if there are $L-L_0(L\ge L_0)$ relays that can effectively eliminate noise, we assume

$$\sigma^2_{R'_1}\to 0^+,\sigma^2_{R'_2}\to 0^+,...,\sigma^2_{R'_{L_0}}\to 0^+, \tag{9}$$

and

$$\sigma^2_{R'_{L_0+1}}>0,\sigma^2_{R'_{L_0+2}}>0,...,\sigma^2_{R'_L}>0. \tag{10}$$

Therefore, the upper bound of $SNR^{\{R_L\}}_{v'_{k_j}\to v_{k_i}}$ is derived as:

$$\frac{\left(\varphi_1(R_{g*})+\sum\limits_{g=1}^{L_0}\varphi_1(R_g)\right)^2}{\left(\varphi_2(R_{g*})\right)^2+\left(\sigma^2_{v_{k_i}}+L_0\sigma^2_{v_{k_i}}\right)^2}. \tag{11}$$

Proof: Please refer to Appendix B.

Lemma 3 Derivation of the upper bound of $\sum\limits_{w=1}^{L}SNR^{R_w}_{v'_{k_j}\to v_{k_i}}$: In view of **Lemma 1**, when multi-path signals have been combined at the receiver v_{k_i}, the upper bound of the total SNR $\max\sum\limits_{w=1}^{L}SNR^{R_w}_{v'_{k_j}\to v_{k_i}}$ for cooperative multiple relays $\{R_L\}$ can be obtained.

Proof: Please refer to Appendix C.

One can see that **Lemma 2** and **Lemma 3** can be implemented in practical scenarios with non-zero noise. At the relays and MECs, we compute and select better relays to increase cooperative diversity, then adopt effective power allocation algorithm to attain the SNR value which is close to the upper bound (see the derived algorithm in **Section III**, **part B**). Based on the above discussions, the SNR upper bound for cooperative multi-path transmission is obtained essentially.

B. Optimal D2D communication based on ultra large scale relays

According to [11, eq. (2)], the channel capacity is given by

$$C=\frac{1}{2}\log_2(1+SNR), \tag{12}$$

where C represents the D2D channel capacity, and SNR is the D2D signal-to-noise ratio. Therefore, the channel capacity of the communication path $v'_{k_j}\to\{R_L\}\to v_{k_i}$ is:

$$C^{\{R_L\}}_{v'_{k_j}\to v_{k_i}}=\frac{1}{2}\log_2(1+SNR^{\{R_L\}}_{v'_{k_j}\to v_{k_i}}). \tag{13}$$

B-1. Uniform Power Allocation: For an arbitrary relay selection subset $\{R_L\}$, if the total power is Q_{tot}, and the power of each relay is constant, the channel capacity $C^{\{R_L\}}_{v'_{k_j}\to v_{k_i}}$ is limited by:

$$Q_{R_1}=Q_{R_2}=\cdots=Q_{R_L}=\frac{Q_{tot}}{L}. \tag{14}$$

B-2. Optimal Relay Selection with Uniform Power: Unlike the arbitrary relay selection in **B-1**, considering the constraints imposed by relay characteristics (e.g., location, fading coefficients, bit error rate), the D2D channel capacity of each relay may vary. We re-arrange the relays in the subset $\{R_{N_{tot}}\}$ ($\{R_L\}\subseteq\{R_{N_{tot}}\}$) in descending order of their individual channel capacities, denoted as $\{R_{opt-N_{tot}}\}=(R_{opt-1},R_{opt-2},\ldots,R_{opt-N_{tot}})$, such that:

$$C^{R_{opt-1}}_{v'_{k_j}\to v_{k_i}}\ge C^{R_{opt-2}}_{v'_{k_j}\to v_{k_i}}\ge\cdots\ge C^{R_{opt-N_{tot}}}_{v'_{k_j}\to v_{k_i}}, \tag{15}$$

where

$$C^{R_{opt-w}}_{v'_{k_j}\to v_{k_i}}=\frac{1}{2}\log_2(1+SNR^{R_{opt-w}}_{v'_{k_j}\to v_{k_i}}). \tag{16}$$

We select the L optimal relays from $\{R_{N_{tot}}\}$ to form $\{R_{opt-L}\}=(R_{opt-1},R_{opt-2},\ldots,R_{opt-L})$, and compute $C^{\{R_{opt-L}\}}_{v'_{k_j}\to v_{k_i}}$.

B-3. Optimal Relay Selection with Optimized Power Allocation: Building upon **B-1** and **B-2**, cooperative transmission introduces interference due to antennas, duplexing, and mutual interference. Therefore, it is essential to allocate the total power more effectively among the selected optimal relays. For the selected set $\{R^*_{opt-L}\}$, we assume that the corresponding power subset is $\{Q^*_{opt-L}\}=(Q^*_{opt-1},Q^*_{opt-2},\ldots,Q^*_{opt-L})$ and total power is Q_{tot}. Each selected relay requires a minimum power for signal forwarding, denoted as $(Q_1,Q_2,\ldots,Q_L)$ $(Q_1>0,Q_2>0,\ldots,Q_L>0)$, such that:

$$C^{R^*_{opt-1}}_{v'_{k_j}\to v_{k_i}}\ge C^{R^*_{opt-2}}_{v'_{k_j}\to v_{k_i}}\ge\cdots\ge C^{R^*_{opt-L}}_{v'_{k_j}\to v_{k_i}}, \tag{17}$$

with

$$Q^*_{opt-1}\ge Q_1,Q^*_{opt-2}\ge Q_2,\ldots,Q^*_{opt-L}\ge Q_L, \tag{18}$$

and

$$\sum_{w=1}^{L}Q^*_{opt-w}=Q_{tot}. \tag{19}$$

In summary, optimal relay selection and efficient power allocation based on real-time computations of relay features are crucial. For the subset $\{R^*_{opt-L}\}$ with non-uniform power allocation ($Q^*_{R_1} \neq Q^*_{R_2} \neq \ldots \neq Q^*_{R_L}$), we have:

$$C^{\{R^*_{opt-L}\}}_{v_{k_i} \to v'_{k_j}} \geq C^{\{R_{opt-L}\}}_{v'_{k_j} \to v_{k_i}} \geq C^{\{R_L\}}_{v'_{k_j} \to v_{k_i}}. \tag{20}$$

IV. D2D COMMUNICATION WITH MEC EQUIPMENTS SUBSETS

A. Optimal correspondence among vehicles and MEC equipments

In Fig. 2, when vehicles in source ($\{V_{sou}\}$), vehicles in destination ($\{V'_{des}\}$) and cooperative mobile relays are selected, we propose an algorithm for MEC subsets selection to further assist D2D communication. We assume that there are q MECs in subset $\{M_q\}(\{M_q\} = (M_1, M_2, ..., M_q))$. Supposing that MEC M_i is corresponds vehicles $\{V_{M_i}\}$, then we have

$$M_i \leftrightarrow \{V_{M_i}\} (\{V_{M_i}\} \subseteq \{V_{sou}\} \cup \{V'_{des}\}), \tag{21}$$

where

$$\{V_{sou}\} \cup \{V'_{des}\} = \bigcup_{i=1}^{q} \{V_{M_i}\}. \tag{22}$$

Based on discussion above, we can optimize real-time vehicle-to-vehicle (V2V) communication by means of cooperative mobile relays and multiple MECs at the same time.

B. D2D communication with MEC subsets for ultra massive vehicles to single vehicle

At certain time-slot, sensing vehicles (subset $\{V'_{des}\}$) detect surrounding real-time information with vehicle motion sensors, and forward it to single moving vehicle v_{k_i} that will move into a geographical area which contains $\{V'_{des}\}$ in a planned way. Hence, we establish communication for multiple vehicles to single vehicle with cooperative mobile relays. We assume that there are k_2 vehicles in $\{V'_{des}\}(\{V'_{des}\} = (v'_1, v'_2, ..., v'_{k_2}))$, $\forall v'_i \subseteq \{V'_{des}\}(1 \leq i \leq k_2)$, v'_i sends information to v_{k_i} with selected L_i relays. Thus $\{V'_{des}\}$ sends information to v_{k_i} with different relays subsets $(\left\{R^{v'_1}_{L_1}\right\}, \left\{R^{v'_2}_{L_2}\right\}, ..., \left\{R^{v'_{k_2}}_{L_{k_2}}\right\})$. If $(v'_1, v'_2, ..., v'_{k_2})$ send detected signals $(y_{v'_1}, y_{v'_2}, ..., y_{v'_{k_2}})$ respectively to v_{k_i}, for vehicle v'_w $(1 \leq w \leq k_2)$, we obtain (23).

Similar to (1) - (3), we obtain the SNR of vehicles-to-vehicle for real-time information transmission in (24). When v_{k_i} receives real-time sensing information, in order to process the total sensing information of destination area for $\{V'_{des}\}$, we assume size each data block size for $(y_{v'_1}, y_{v'_2}, ..., y_{v'_{k_2}})$ is the same. Therefore, we evaluate the lower bound of channel capacity for $\{V'_{des}\} \to v_{k_i}$ as

$$\arg\sup \left(C^{\left\{R^{v'_1}_{L_1}\right\}}_{v'_1 \to v_{k_i}}, C^{\left\{R^{v'_2}_{L_2}\right\}}_{v'_2 \to v_{k_i}}, ..., C^{\left\{R^{v'_{k_2}}_{L_{k_2}}\right\}}_{v'_{k_2} \to v_{k_i}} \right). \tag{25}$$

On the other hand, by selecting MECs, we derive communication process for $\{V'_{des}\} \to \{M_q\} \to v_{k_i}$ to aid vehicles-to-vehicle communication. We assume v_{k_i} is associated to MEC equipment M_i and $\{V'_{des}\}$ is associated to MEC M_{i+1}. Therefore we establish communication as $\{V'_{des}\} \leftrightarrow M_{i+1} \to M_i \leftrightarrow v_{k_i}$.

C. D2D channel capacity upper bound with MEC subsets

We assume that the fading channels coefficients are respectively $(h_{v'_1 M_{i+1}}, h_{v'_2 M_{i+1}}, ..., h_{v'_{k_2} M_{i+1}})$, $h_{M_{i+1} M_i}$ and $h_{M_i v_{k_i}}$ for $(v'_1, v'_2, ..., v'_{k_2}) \to M_{i+1}$, $M_{i+1} \to M_{i+1}$ and $M_i \to v_{k_i}$. The power levels of M_i and M_{i+1} are Q_{M_i} and $Q_{M_{i+1}}$, the noise variances of M_i, M_{i+1} and v_{k_i} are respectively $\sigma^2_{M_{i+1}}$, $\sigma^2_{M_i}$ and $\sigma^2_{v_{k_i}}$. At the receiver v_{k_i}, the maximum ratio combining (MRC) is adopted. At the first time-slot, for receiver M_{i+1}, we have:

$$y_{\{V'_{des}\} \to M_{i+1}} = \sum_{q=1}^{k_2} \sqrt{Q_{v'_q}} h_{v'_q M_{i+1}} y_{v'_q} + \sigma^2_{M_{i+1}}, \tag{26}$$

At the second time-slot, for receiver M_i, we have:

$$y_{M_{i+1} \to M_i} = \sqrt{Q_{M_{i+1}}} h_{M_{i+1} M_i} y_{\{V'_{des}\} \to M_{i+1}} + \sigma^2_{M_i}. \tag{27}$$

At the third time-slot, for receiver v_{k_i}, we have:

$$y_{M_i \to v_{k_i}} = \sqrt{Q_{M_i}} h_{M_i v_{k_i}} y_{M_{i+1} \to M_i} + \sigma^2_{v_{k_i}}. \tag{28}$$

Combined with above equations, $\{V'_{des}\} \leftrightarrow M_{i+1} \to M_i \leftrightarrow v_{k_i}$ is shown in (29). Since $y_{v'_q}$ is the desired signal and channels of relays are different from that of MECs, it is noteworthy that the perceptual capability of each vehicle remains the same in general, and the perceptual data block also remains the same for each vehicle in the fixed time. Therefore, the maximum D2D SNR for MEC communication is shown in (30).

Hence, at the receiver v_{k_i}, we adopt MRC to combine D2D SNR for relay subsets and MEC subsets. Therefore, the total channel capacity of $\{V'_{des}\} \to v_{k_i}$ can be expressed as:

$$C_{\{V'_{des}\} \to v_{k_i}} = \frac{1}{2} \log_2(1 + SNR_A + SNR_B), \tag{31}$$

where:

$$\begin{cases} SNR_A = SNR^{\bigcup_{w=1}^{k_2} \left\{R^{v'_w}_{L_w}\right\}}_{\{V'_{des}\} \to v_{k_i}} \\ SNR_B = SNR^{M_{i+1} \cup M_i}_{\{V'_{des}\} \to v_{k_i}}. \end{cases} \tag{32}$$

D. D2D latency analysis

In practical communication system, transmission delay τ is defined in (33). When communication entities are determined in some time-slot, if block size, channel length, speed of radio waves, queue time of data packets and data processing time are constants, the transmission delay $\tau_{\{V'_{des}\} \to v_{k_i}}$ for $\{V'_{des}\} \to v_{k_i}$ satisfies the following condition:

$$\tau_{\{V'_{des}\} \to v_{k_i}} \propto \frac{1}{C_{\{V'_{des}\} \to v_{k_i}}}. \tag{34}$$

In this work, we mainly investigate upper bound of D2D channel capacity and effective sensing information fusion. From (34), it is shown that when D2D channel capacity increases, transmission delay decreases accordingly.

$$y_{v'_w \to v_{k_i}}^{\left\{R_{L_w}^{v'_w}\right\}} = \sum_{g=1}^{L_w} \left(\sqrt{Q_{R_g}} h_{R_g v_{k_i}} \sqrt{Q_{v'_w}} h_{v'_w R_g} y_{v'_w} + \sqrt{Q_{R_g}} h_{R_g v_{k_i}} \sigma_{R_g}^2\right) + L_w \sigma_{v_{k_i}}^2. \tag{23}$$

$$\mathbf{SNR}_{\mathbf{v'_w \to v_{k_i}}}^{\left\{\mathbf{R_{L_w}^{v'_w}}\right\}} = \frac{\left| \sqrt{\mathbf{Q}_{\left\{\mathbf{R_{L_w}^{v'_w}}\right\}}} \circ \mathbf{h}_{\left\{\mathbf{R_{L_w}^{v'_w}}\right\}\mathbf{v_{k_i}}} \circ \sqrt{\mathbf{Q}_{\mathbf{v'_w}}} \circ \mathbf{h}_{\mathbf{v'_w}\left\{\mathbf{R_{L_w}^{v'_w}}\right\}} \right|^{\mathbf{2}}}{\left| \sqrt{\mathbf{Q}_{\left\{\mathbf{R_{L_w}^{v'_w}}\right\}}} \circ \mathbf{h}_{\left\{\mathbf{R_{L_w}^{v'_w}}\right\}\mathbf{v_{k_i}}} \circ \boldsymbol{\sigma}^{\mathbf{2}}_{\left\{\mathbf{R_{L_w}^{v'_w}}\right\}} \right|^{\mathbf{2}} + \left|\boldsymbol{\sigma}^{\mathbf{2}}_{\mathbf{v_{k_i}}}\right|^{\mathbf{2}}} \circ |\mathbf{y_{v'_w}}|^{\mathbf{2}}. \tag{24}$$

$$y_{M_i \to v_{k_i}} = \sqrt{Q_{M_i} Q_{M_{i+1}}} h_{M_i v_{k_i}} h_{M_{i+1} M_i} \left(\sum_{q=1}^{k_2} \sqrt{Q_{v'_q}} h_{v'_q M_{i+1}} y_{v'_q} + \sigma_{M_{i+1}}^2\right) + \sqrt{Q_{M_i}} h_{M_i v_{k_i}} \sigma_{M_i}^2 + \sigma_{v_{k_i}}^2. \tag{29}$$

$$SNR_{\{V'_{des}\} \to v_{k_i}}^{M_{i+1} \cap M_i} = \sup \frac{|\sqrt{Q_{M_i}} h_{M_i v_{k_i}} \sqrt{Q_{M_{i+1}}} h_{M_{i+1} M_i} \min \sum_{q=1}^{k_2} \sqrt{Q_{v'_q}} h_{v'_q M_{i+1}} \mathrm{y}_{v'_q}|^2}{|\sqrt{Q_{M_i}} h_{M_i v_{k_i}} \sqrt{Q_{M_{i+1}}} h_{M_{i+1} M_i} \sigma_{M_{i+1}}^2|^2 + \left|\sqrt{Q_{M_i}} h_{M_i v_{k_i}} \sigma_{M_i}^2\right|^2 + \left|\sigma_{v_{k_i}}^2\right|^2}. \tag{30}$$

Algorithm 1 Real-time Communication for Multiple Perceptual Vehicles $\{V'_{\text{des}}\}$ to Single Vehicle v_{k_i} in 6G Ultra-Large-Scale C-V2X Networks

1: In certain successive time-slots, vehicle $v_{k_i} \in \{V_{\text{sou}}\}$ forecasts surrounding traffic areas that it will travel through, and identifies a critical vehicle subset $\{V'_{\text{des}}\}$ to establish communication.
2: **for** each vehicle $v'_i \in \{V'_{\text{des}}\}$ **do**
3: Compute and select optimal L_i cooperative mobile relays.
4: Transmit perceptual information to vehicle v_{k_i}.
5: Search for optimal corresponding MEC to support D2D communication in the new path.
6: **end for**
7: With selected MEC equipment, v'_i and $\{V'_{\text{des}}\}$ jointly compute to optimize dynamic vehicle-to-vehicle communication over different time intervals.

V. Effective information estimation for multiple vehicles to single vehicle

A. Minimal subsets for cooperative mobile relays and MEC equipments

In certain area, we divide the traffic information into three classes. The first class contains slow changing traffic information, such as fixed buildings, trees, road facilities, etc. The second class contains fast changing traffic information that vehicles can sense. For example in the perceptual range of moving vehicles, one can sense moving vehicles, pedestrians, mobile IoT devices, and structures that are under construction. The third class contains fast changing traffic information that is out of perceptual range of moving vehicles $\{V'_{des}\}$. At certain time-slot, because of a limited number of moving persons and objects, the total information of that area is assumed to be fixed. Hence, for the second class fast changing traffic information, v_{k_i} selects vehicles subset $\{V'_{des}\}$ to obtain real-time information. Since v'_1, v'_2,..., v'_{k_2} are independent from each other, if relay subset of v'_i with L relays is $\{R_L^{v'_i}\}$, we have minimal cooperative mobile subset as $\bigcup_{i=1}^{k_2} \left\{R_{L_i}^{v'_i}\right\}$. Similarly, for D2D communication $\{V'_{des}\} \to \{V_{sou}\}$ ($v'_{k_j} \subseteq \{V'_{des}\}, v_{k_i} \subseteq \{V_{sou}\}$), we assume that v'_{k_j} is associated to $MEC_{v'_{k_j}}$, v_{k_i} is associated to $MEC_{v_{k_i}}$, minimal MEC subsets are expressed as $\bigcup_{i=1}^{k_2} \bigcup_{j=1}^{k_1} \left\{MEC_{v'_i}, MEC_{v_j}\right\}$. Therefore we obtain minimal subsets of cooperative mobile relays and MECs for optimal D2D communication.

B. Effective information estimation algorithm for integrated sensing and communication

In view of the total information classification discussed above, we assume that the total information of the area that v_{k_i} will travel into contain three classes: the first class is the slow-changing traffic information, the second class is the fast-changing traffic information that vehicles can sense, the third class is the fast-changing traffic information that is out of perceptual range. Since we mainly investigate optimal sensing information fusion from destination vehicles subset $\{V'_{des}\}$ to source vehicles subset $\{V_{sou}\}$, we just discuss the second class information-fast changing traffic information which vehicles sense and transmit to v_{k_i} in real-time in real-time.

Therefore, we investigate sensing and transmission process of $\{V'_{des}\}$ and assume that total real-time sensing information is $\text{Inf}_{\{V'_{des}\}}$. At some time-slot, as sensing information for $(v'_1, v'_2, ..., v'_{k_2})$ is expressed as $(\text{Inf}_{v'_1}, \text{Inf}_{v'_2}, ..., \text{Inf}_{v'_{k_2}})$ respectively, if $\text{Inf}_{v'_1}$, $\text{Inf}_{v'_2}$,..., and $\text{Inf}_{v'_{k_2}}$ are independent and they are not intersected with each other, the total real-time information is defined as

$$\text{Inf}_{\{V'_{des}\}} = \sum_{i=1}^{k_2} \text{Inf}_{v'_i}. \tag{35}$$

$$\tau = \frac{\text{block size}}{\text{channel capacity}} + \frac{\text{channel length}}{\text{speed of radio waves}} + \text{queue time of data packets} + \text{data process time}. \quad (33)$$

On the other hand, in general case if $\mathrm{Inf}_{v'_1}$, $\mathrm{Inf}_{v'_2}$,..., and $\mathrm{Inf}_{v'_{k_2}}$ are intersected, we divide $(v'_1, v'_2, ..., v'_{k_2})$ into n subsets, in which elements are intersected with each other and elements in different subsets are independent. Assuming that the numbers of n subsets are N_1, N_2,..., N_n $(k_2 = \sum_{i=1}^{n} N_i)$, we have:

$$\{V'_{des}\} = (\{V'_{sub1-N_1}\}, \{V'_{sub2-N_2}\}, ..., \{V'_{subn-N_n}\}). \quad (36)$$

whereby the $i-th$ subset with N_i vehicles is

$$\{V'_{subi-N_i}\} = (v'_{subi-1}, v'_{subi-2}, ..., v'_{subi-N_i}). \quad (37)$$

The sensing information of $\{V'_{subi-N_i}\}$ can be expressed as:

$$\mathrm{Inf}_{\{V'_{subi-N_i}\}} = (\mathrm{Inf}_{v'_{subi-1}}, \mathrm{Inf}_{v'_{subi-2}}, ..., \mathrm{Inf}_{v'_{subi-N_i}}). \quad (38)$$

Since $\mathrm{Inf}_{v'_{subi-1}}$, $\mathrm{Inf}_{v'_{subi-2}}$,..., and $\mathrm{Inf}_{v'_{subi-N_i}}$ are not independent, the total information of $\{V'_{subi-N_i}\}$ can be written as:

$$\mathrm{Inf}_{\{V'_{subi-N_i}\}} = \bigcup_{k=1}^{N_i} \mathrm{Inf}_{v'_{subi-k}}. \quad (39)$$

With the aid of the inclusion-exclusion principle, $\bigcup_{k=1}^{N_i} \mathrm{Inf}_{v'_{subi-k}}$ is derived as (40). To sum up, for $\{V'_{des}\}$ with $n\,(n \in N^*)$ independent subsets, the total information is derived as eq. (41).

Algorithm 2 Effective Information Estimation for Moving Vehicle v_{k_i}

1: Based on **Algorithm 1**, vehicle v_{k_i} and the set of vehicles $(v'_1, v'_2, \ldots, v'_{k_2})$ construct an intelligent IoE, and compute minimal subsets of cooperative relays and MEC equipment to achieve optimal D2D communication.
2: Vehicles $(v'_1, v'_2, \ldots, v'_{k_2})$ sense and transmit surrounding second-class information to v_{k_i} in real time.
3: Vehicle v_{k_i} senses first-class and third-class information and receives second-class perceptual information to derive $\mathrm{Inf}_{\mathrm{tot}}$.

VI. Simulations

In this section, we present simulation results for the proposed algorithms. Simulation conditions are similar to those in [9]-[14], [21], [25], [26], whereby we consider ultra large-scale V2X networks with multiple relays for D2D communication. Similar to [9-14], we assume that the total number of relays is 50. In order to present dynamic C-V2X mobile network feature, power allocation and channel fading coefficients between relays and vehicles keep changing from one time slot to another (**Section VI. A, B**, (42) and (43)). To compare our proposed schemes with the existing ones, it is assumed that there is a bandwidth of 1 kbps for the channel capacity, channel fading coefficients are belong to a certain range, and flexible power allocation is adopted to both the device subsets and relay subsets.

Our objective is to demonstrate the advantages of multiple relay selection for V2V communication, and illustrate the theoretical principle of optimal communication in 6G ultra-large-scale V2X networks. Based on the proposed **Algorithm 1** and **Algorithm 2**, our numerical simulations show that the number of selected relays can not be too large, and an excessive number of selected relays and inappropriate power allocation can significantly degrade the communication performance. Therefore, up to a total of 20 selected relays are considered. We also analyze the sensing characteristics of MM-wave radars in vehicle networks and show that information evaluation theory can significantly reduce the computational complexity for real-time total sensing information.

A. Optimal Communication with Ultra-Large-Scale Relays

We first evaluate the optimal communication for V2V links based on ultra large-scale relays. Consider an arbitrary mobile relay R_g which is contained in relay subset with total relays number 100. If R_g moves towards v'_{k_j}, we set the channel coefficients $h_{v'_{k_j}R_g} \in [0.8, 0.95]$ and $h_{R_g v_{k_i}} \in [0, 0.65]$. If R_g moves towards v_{k_i}, we set $h_{v'_{k_j}R_g} \in [0.75, 0.9]$ and $h_{R_g v_{k_i}} \in [0, 0.7]$. In Fig. 3 and Fig. 4, we assume $|y_{v'_{k_j}}(t)|^2 = 2$ and $\sigma^2_{v_{k_i}} = \sigma^2_{R_g} = 1$. Following transmit power range for each antenna (5 *W*-25 *W*) as reported in [3], [7], [9], [10], [12], [13], we set $Q_{v'_{k_j}} = 15$ *W* and the average $Q_{R_g} = 20$ *W* in Fig. 3.

In Fig. 3, we evaluate the channel capacity versus the number of relays for the fading channel coefficient interval values of $d = 0.001$ and $d = 0.004$. The results show that as the number of relays increases, the channel capacity improves, and a larger d corresponds to a higher channel capacity. This is due to the multi-relay diversity provided by multiple relays, and the necessity of appropriate fading coefficient values for increasing channel capacity. Furthermore, we observe that with an average $Q_{R_g} = 20$ *W* (where the total power of relays increases with the number of relays), higher transmit rates are achieved with the optimal solution. This is because relays with higher d values are selected.

Based on the observations in Fig. 3, in Fig.4 we investigate the channel capacity changes when Q_{R_g} is not constant and $Q_{v'_{k_j}} = 15$ *W*, 20 *W*. Our simulation results indicate that the power value of the source $Q_{v'_{k_j}}$ is more critical than the power value of the relays Q_{R_g}. Therefore, we should prioritize allocating more power to $Q_{v'_{k_j}}$ when selecting optimal relay subsets.

$$\bigcup_{k=1}^{N_i} \mathrm{Inf}_{v'_{subi-k}} = \sum_{l=1}^{N_i} (-1)^{l-1} \sum_{1\le m_1<m_2<\ldots<m_k\le N_i} \mathrm{Inf}_{v'_{subi-m_1}} \cap \mathrm{Inf}_{v'_{subi-m_2}} \cap \ldots \cap \mathrm{Inf}_{v'_{subi-m_k}}. \quad (40)$$

$$\mathrm{Inf}_{\{V'_{des}\}} = \bigcup_{i=1}^{n} \sum_{l=1}^{N_i} (-1)^{l-1} \sum_{1\le m_1<m_2<\ldots<m_k\le N_i} \mathrm{Inf}_{v'_{subi-m_1}} \cap \mathrm{Inf}_{v'_{subi-m_2}} \cap \ldots \cap \mathrm{Inf}_{v'_{subi-m_k}}. \quad (41)$$

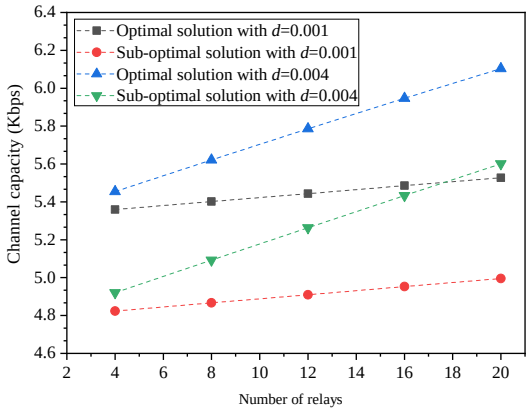

Fig. 3. Channel capacity versus number of relays when number of relays is 100, $Q_{\mathrm{sou}} = 18\ W$

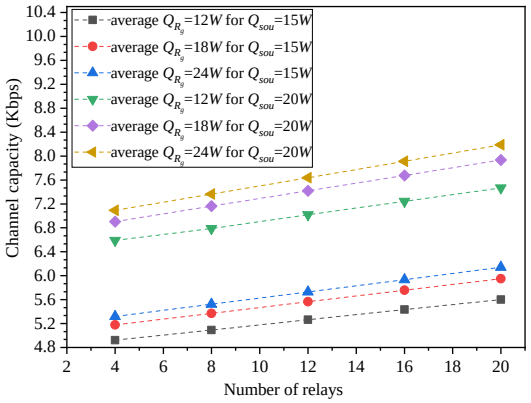

Fig. 4. Channel capacity versus the number of relays for algorithms comparison

B. Comparison with Existing Algorithms

Building upon the results in Fig. 3 and Fig. 4, we further analyze our proposed algorithm and compare it with existing algorithms. Similar to [8], [9], [12] - [14], we consider cooperative C-V2X scenarios with pseudorandom vehicle distribution at a given time slot. We set $Q_{v'_{k_j}} = 18\ W$, $|y_{v'_{k_j}}|^2 = 2$, $h_{v'_{k_j}R_g} \in [0.5, 0.9]$, $h_{R_g v_{k_i}} \in [0, 0.7]$, $d = 0.004$, $Q_{R_g} \in [10\ \ W, 25\ \ W]$, $\sigma^2_{R_g} = 1$ for $g \equiv 1, 2 \pmod 3$, $\sigma^2_{R_g} = 0$ for $g \equiv 0 \pmod 3$, and $\sigma^2_{v_{k_i}} = 2$. For the algorithm in [12], relays are selected based on higher fading coefficients. For the algorithm in [13], relays are selected based on larger power values with constant and different fading coefficients.

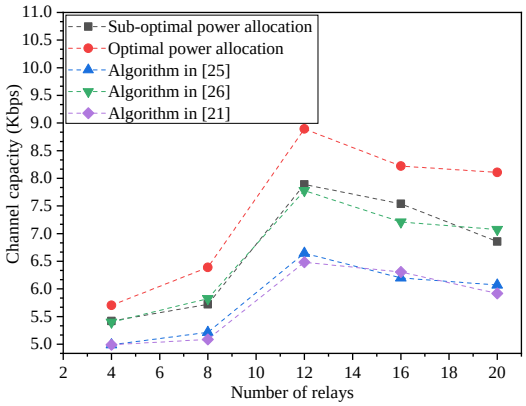

Fig. 5. Channel capacity versus number of relays when number of relays is 100, Q_{R_g} is constant

Fig. 5 shows that our proposed algorithm achieves a 0.8-2.5 *Kbps* higher channel capacity compared to that in [9], [12], [13]. (Algorithms in [8], [14] have similar models to [9], [12], [13], so we only compare with [9], [12], [13]) This is because we comprehensively consider various relay types, compute optimal and sub-optimal channel capacities, and then select better relays from various vehicle subsets. In contrast, the algorithms in [9], [12], [13] only consider one or partial relay types and do not present an optimal power allocation scheme.

Interestingly, we observe that increasing relay diversity does not always yield a higher channel capacity. In Fig. 5, the channel capacity decreases when the number of relays exceeds 12. This is because the noise from some relays has a greater impact than their signals when signals are combined at the receiver v_{k_i}, resulting in a smaller total SNR. The descending rate also varies among different algorithms.

On the other hand, we evaluate D2D channel capacity with MEC (because we have compared our algorithm with other core C-V2X algorithms, we just simulate our scheme in Fig. 6 and Fig. 7). We assume that the number of total MECs is 75, $Q_{MEC_{v'_i}} = Q_{MEC_{v_j}} = 20\ W$. In order to present optimal selection for MECs, we further assume that

$$h_{v'_q M_{i+1}} h_{M_{i+1} M_i} h_{M_i v_{k_i}} = 0.7, \quad (42)$$

with

$$h_{v'_q M_{i+1}}, h_{M_{i+1} M_i}, h_{M_i v_{k_i}} \in [0.7, 1]. \quad (43)$$

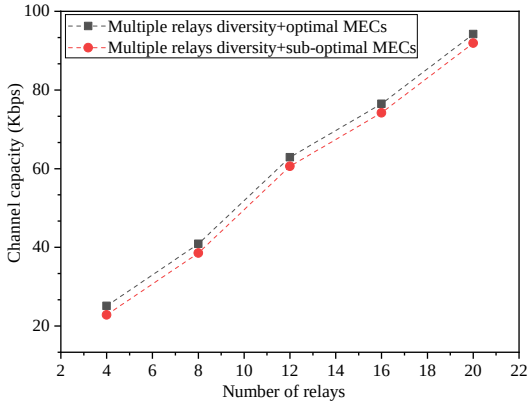

Fig. 6. Channel capacity versus number of relays for multiple relays diversity with MECs

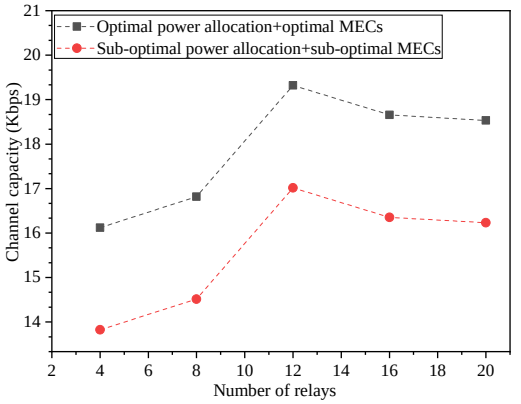

Fig. 7. Channel capacity versus number of relays for power allocation with MECs

From Fig. 6 and Fig. 7, it is concluded that we can continuously improve channel capacity by adopting signal separation at the receiver v_{k_i}. Furthermore, optimal/sub-optimal MEC algorithm does not improve the channel capacity when the number of relays is more than 12. Besides, it is found that our proposed MEC algorithm is approximately 2.5 *Kbps* higher than the sub-optimal MEC algorithm.

In Fig. 8, we evaluate the computation complexity versus the number of relays for the proposed low-complexity selection algorithm. It is assumed that number of relay subset $(\{R_S\} = (R_1, R_2, ..., R_S))$ is S, the number of relay types in R_k is $m_{R_k}(m_{R_k} \in N^*)$. One can show that the computation complexity can be expressed as follows:

$$\begin{cases} \log_2({m_k}^{m_k} + (S - m_k)^{m_k}), & \text{if} \quad m_k < S \\ \log_2(S^{m_k}), & \text{if} \quad m_k \geq S. \end{cases} \tag{44}$$

As shown in Fig. 8, when the total number of relays types is 8, the computation complexity of the proposed algorithm is nearly half ($\mathrm{m}_k = 5$) and one fourth ($\mathrm{m}_k = 2$) of that of the exhaustive search method. This is because we consider

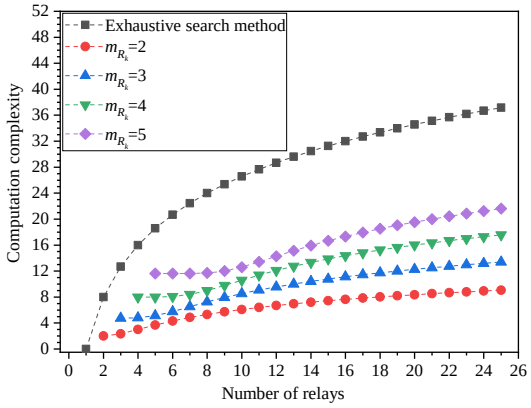

Fig. 8. Computation complexity versus number of relays for proposed low complexity selection algorithm

selecting more effective relay types and relay subsets, thus leading to improved channel capacity with less selection times.

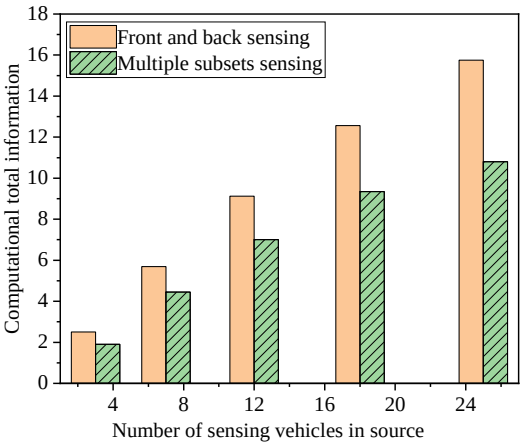

Fig. 9. Computational total information versus number of sensing vehicles for five vehicles subsets (3,4,5,6,7)

Lastly, we present integrated sensing computation for $\{V_{sou}\}$ with MM-wave radars. There are three types of MM-wave radars (240 *Km/h*) for vehicular networks, including long-distance range radars (LRR, perception range is 10 *m* - 200 *m*), middle-distance range radars (MRR, perception range is 1 *m* - 100 *m*) and small-distance range radars (SRR, perception range is 0.5 *m* - 30 *m*). We assume that the total number of vehicles in $\{V'_{des}\}$ is k_2, which can be expressed as:

$$k_2 = \sum_{i=1}^{J} k_{2i}. \tag{45}$$

where $k_{21}, k_{22}, ..., k_{2J} \in N^*$, for k_2 sensing vehicles. By calculating the total joint sensing information, the NETs can

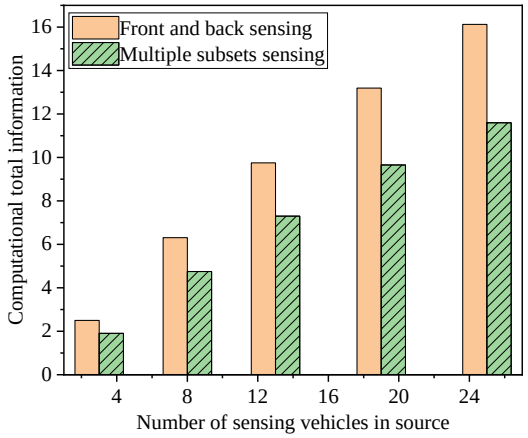

Fig. 10. Computational total information versus the number of sensing vehicles for five vehicles subsets (3,5,5,6,6)

be expressed as :

$$\sum_{i=1}^{k_2} C_{k_2}^{i}. \tag{46}$$

where $C_{k_2}^{i} = (k_2!)/(i!(k_2-i)!)$. However, in practice, the total sensing information is not uniformly distributed. Therefore, in order to better perceive critical area information and reduce NETs, the total sensing information is divided by J partial sensing information, and the NETs are reduced to:

$$\sum_{j=1}^{J} \sum_{i=1}^{k_{2j}} C_{k_{2j}}^{i}. \tag{47}$$

Clearly, the NETs in (46) are far less than that in (47). To have lower NETs, we assume that sensing capabilities remain the same for each vehicle, and sensing information of each vehicle is 1, the total number of vehicles is 25 and the number of vehicles subsets are (3,4,5,6,7) and (3,5,5,6,6) (we will compare computational total information in Fig. 9 and Fig. 10 for different NETs). Consequently, we simulate multiple moving vehicles sensing with two cases:

1) Sparse vehicles scenario (block diagram in Fig. 9 and Fig. 10). We propose front and back sensing method to evaluate information of adjacent vehicles. Distances of adjacent vehicles for five vehicles subsets are respectively 150 *m*, 125 *m*, 100 *m*, 75 *m* and 50 *m*.
2) Dense vehicles scene (block diagram with slants in Fig. 9 and Fig. 10). We propose multiple subsets sensing method to evaluate information of multiple vehicles. Minimal distances of arbitrary two vehicles for five vehicles subsets are 100 *m*, 80 *m*, 60 *m*, 40 *m* and 20 *m*, interval distance increment is 20 *m*.

Computational total information with (3,4,5,6,7) and (3,5,5,6,6) are respectively simulated in Fig. 9 and Fig. 10. If we compute all vehicles 25 at the same time, NETs of front and back sensing/multiple subsets sensing are 49/325, for (3,4,5,6,7) NETs of front and back sensing/multiple subsets sensing are just 44/80, and for (3,5,5,6,6) NETs of front and back sensing/multiple subsets sensing are just 45/78. This shows that if we take front and back sensing in spare vehicles scenario, NETs almost never change. However, we take multiple subsets sensing in dense vehicles case, we shall find critical multiple areas with corresponding vehicles, and NETs will be reduced as low as possible. On the other hand, combined with Fig. 9 and Fig. 10, for better perceptual accuracy, one needs to increase total computation information and NETs to coordinate cooperative sensing of multiple vehicles. Therefore it is important to weigh computational total information against NETs under conditions of perceptual accuracy in 6G C-V2X networks.

VII. Conclusion

This work has presented a novel framework for optimal real-time communication and efficient information evaluation tailored for vehicle-to-vehicle in 6G ultra-large-scale C-V2X networks. By leveraging intelligent relays selection and MEC equipments coordination, the proposed algorithms significantly outperform existing cooperative vehicular methods in terms of channel capacity while maintaining exceptionally low computational complexity. We analytically establish the existence of an upper bound on D2D channel capacity based on inequality and functional mapping theories, and introduce a scalable multi-class relays selection mechanism. In addition, an effective information estimation theory has been derived for vehicles equipped with mmWave radar systems to enhance cooperative perception. These contributions lay a solid theoretical and algorithmic foundation for future developments in 6G-enabled real-time communication, dynamic map construction, and large-scale C-V2X systems.

In addition, security is a fundamental challenge in 6G cooperative relays communication. As a future work, we plan to consider message dissemination latency, latency, eavesdropping, and tampering.

Appendix A
Proof of **Lemma 1**

From (1) and(2), the received signal at v_{k_i} via the relays $\{R_L\}$ is given by (48). The SNR for the combined path is expressed as:

$$SNR_{v'_{k_j}\to v_{k_i}}^{\{R_L\}} = \frac{\left(\sum\limits_{g=1}^{L} \sqrt{Q_{R_g}} h_{R_g v_{k_i}} \sqrt{Q_{v'_{k_j}}} h_{v'_{k_j} R_g} y_{v'_{k_j}}\right)^2}{\left(\sum\limits_{g=1}^{L} \sqrt{Q_{R_g}} h_{R_g v_{k_i}} \sigma_{R_g}\right)^2 + (L\sigma_{v_{k_i}}^2)^2}. \tag{49}$$

When $\sigma_{v_{k_i}}^2 = 0$, (49) simplifies to:

$$SNR_{v'_{k_j}\to v_{k_i}}^{\{R_L\}} = \frac{\left(\sum\limits_{g=1}^{L} \sqrt{Q_{R_g}} h_{R_g v_{k_i}} \sqrt{Q_{v'_{k_j}}} h_{v'_{k_j} R_g} y_{v'_{k_j}}\right)^2}{\left(\sum\limits_{g=1}^{L} \sqrt{Q_{R_g}} h_{R_g v_{k_i}} \sigma_{R_g}\right)^2}. \tag{50}$$

$$y_{v'_{k_j}\to v_{k_i}}^{\{R_L\}} = \sum_{g=1}^{L}\left(\sqrt{Q_{R_g}}h_{R_g v_{k_i}}\sqrt{Q_{v'_{k_j}}}h_{v'_{k_j}R_g}y_{v'_{k_j}} + \sqrt{Q_{R_g}}h_{R_g v_{k_i}}\sigma_{R_g}\right) + L\sigma^2_{v_{k_i}}. \tag{48}$$

On the other hand, when $\sigma^2_{v_{k_i}} = 0$, the sum of the individual SNRs is given by (51).

Define:

$$\begin{cases} U_w = \left|\sqrt{Q_{R_w}}h_{R_w v_{k_i}}\sqrt{Q_{v'_{k_j}}}h_{v'_{k_j}R_w}y_{v'_{k_j}}\right| \\ I_w = \left|\sqrt{Q_{R_w}}h_{R_w v_{k_i}}\sigma^2_{R_w}\right|. \end{cases} \tag{52}$$

Then (51) can be written as:

$$\sum_{w=1}^{L} SNR_{v'_{k_j}\to v_{k_i}}^{R_w} = \sum_{w=1}^{L}\frac{U_w^2}{I_w^2}. \tag{53}$$

Since $U_w \geq 0$ and $I_w \geq 0$, let $U_w = u_w I_w$, where u_w is a non-negative real number. Thus,

$$\sum_{w=1}^{L} SNR_{v'_{k_j}\to v_{k_i}}^{R_w} = \sum_{w=1}^{L} u_w^2. \tag{54}$$

Multiplying the numerator and denominator of (54) by $\left(\sum_{w=1}^{L} I_w\right)^2$, we have

$$\sum_{w=1}^{L} SNR_{v'_{k_j}\to v_{k_i}}^{R_w} = \frac{\sum_{w=1}^{L} u_w^2\left(\sum_{w=1}^{L} I_w\right)^2}{\left(\sum_{w=1}^{L} I_w\right)^2}. \tag{55}$$

Expanding $\left(\sum_{w=1}^{L} I_w\right)^2$, we have

$$\left(\sum_{w=1}^{L} I_w\right)^2 = \sum_{w=1}^{L} I_w^2 + 2\sum_{1\leq i,j\leq L, i\neq j} I_i I_j. \tag{56}$$

Therefore, it is clear that

$$\left(\sum_{w=1}^{L} I_w\right)^2 \geq \sum_{w=1}^{L} I_w^2. \tag{57}$$

Using (55) and (57), we obtain:

$$\sum_{w=1}^{L} SNR_{v'_{k_j}\to v_{k_i}}^{R_w} \geq \frac{\sum_{w=1}^{L} u_w^2 \sum_{w=1}^{L} I_w^2}{\left(\sum_{w=1}^{L} I_w\right)^2}. \tag{58}$$

Applying the Cauchy-Schwarz inequality, we have

$$\sum_{w=1}^{L} SNR_{v'_{k_j}\to v_{k_i}}^{R_w} \geq \frac{\left(\sum_{w=1}^{L} u_w I_w\right)^2}{\left(\sum_{w=1}^{L} I_w\right)^2}. \tag{59}$$

Finally, we conclude that the SNR upper bound is

$$SNR_{v'_{k_j}\to v_{k_i}}^{\{R_L\}} \leq \sum_{w=1}^{L} SNR_{v'_{k_j}\to v_{k_i}}^{R_w}. \tag{60}$$

APPENDIX B
PROOF OF LEMMA 2

On one hand, if $\forall R_t \in \{R_L\}$ and $\sigma^2_{R_t} \neq 0$, it is obvious that $\varphi_1(R_t) \geq 0$ and $\varphi_2(R_t) \geq 0$ in (5). We use mathematical induction to derive the conclusion (11).

When $L = 1$, the proposition is evident.

When $L = 2$, $\{R_L\}$ can be expressed as (R_{g*}, R'_1). With the aid of known condition, we have

$$\varphi_1(R_{g*})\varphi_2(R'_1) \geq \varphi_1(R'_1)\varphi_2(R_{g*}). \tag{61}$$

We sum $\varphi_1(R_{g*})\varphi_2(R_{g*})$ at the same time for both sides of inequality and obtain:

$$\varphi_1(R_{g*})(\varphi_2(R_{g*}) + \varphi_2(R'_1)) \geq \varphi_2(R_{g*})(\varphi_1(R_{g*}) + \varphi_1(R'_1)). \tag{62}$$

Because $\varphi_2(R_{g*}) \geq 0$ and $\varphi_2(R_{g*}) + \varphi_2(R'_1) \geq 0$, we have

$$\frac{\varphi_1(R_{g*})}{\varphi_2(R_{g*})} \geq \frac{\varphi_1(R_{g*}) + \varphi_1(R'_1)}{\varphi_2(R_{g*}) + \varphi_2(R'_1)} \tag{63}$$

Combined with (7), $\forall i_1, i_2 (i_1, i_2 \in \mathbf{N}^*)$, if $1 \leq i_1 \leq i_2 \leq L-1$, we conclude that

$$\frac{\varphi_1(R_{g*})}{\varphi_2(R_{g*})} \geq ... \geq \frac{\varphi_1(R_{g*}) + \varphi_1(R'_{L-1})}{\varphi_2(R_{g*}) + \varphi_2(R'_{L-1})}, \tag{64}$$

Thus, for $L = 2$, we have

$$\frac{\varphi_1(R_{i_1})}{\varphi_2(R_{i_1})} \geq \frac{\varphi_1(R_{i_1}) + \varphi_1(R_{i_2})}{\varphi_2(R_{i_1}) + \varphi_2(R_{i_2})}. \tag{65}$$

When $L = 3$, $\{R_L\}$ is expressed as (R_{g*}, R'_1, R'_2), we also have

$$\frac{\varphi_1(R_{g*})}{\varphi_2(R_{g*})} \geq \frac{\varphi_1(R'_2)}{\varphi_2(R'_2)}, \tag{66}$$

With the help of (63) - (66), we obtain:

$$\frac{\varphi_1(R_{g*})}{\varphi_2(R_{g*})} \geq \frac{\varphi_1(R_{g*}) + \varphi_1(R'_1)}{\varphi_2(R_{g*}) + \varphi_2(R'_1)} \geq \frac{\varphi_1(R'_1) + \varphi_1(R'_2)}{\varphi_2(R'_1) + \varphi_2(R'_2)}, \tag{67}$$

Combining with case of $L = 2$, inference for $L = 3$ will be derived as

$$\frac{\varphi_1(R_{g*})}{\varphi_2(R_{g*})} \geq \frac{\varphi_1(R_{g*}) + \varphi_1(R'_1) + \varphi_1(R'_2)}{\varphi_2(R_{g*}) + \varphi_2(R'_1) + \varphi_2(R'_2)}. \tag{68}$$

When $L = N$, $\{R_L\} = (R_{g*}, R'_1, R'_2, ..., R'_{N-1})$, with the aid of conclusions for $L = 1$, $L = 2$,..., and $L = N-1$, we have

$$\frac{\varphi_1(R_{g*})}{\varphi_2(R_{g*})} \geq \frac{\sum_{p=1}^{N-1}\varphi_1(R'_p)}{\sum_{p=1}^{N-1}\varphi_2(R'_p)}, \tag{69}$$

Also with the aid of (6), we obtain

$$\frac{\varphi_1(R_{g*})}{\varphi_2(R_{g*})} \geq \frac{\varphi_1(R_{g*}) + \sum_{p=1}^{N-1}\varphi_1(R'_p)}{\varphi_2(R_{g*}) + \sum_{p=1}^{N-1}\varphi_2(R'_p)}. \tag{70}$$

$$\sum_{w=1}^{L} SNR_{v'_{k_j}\to v_{k_i}}^{R_w} = \sum_{w=1}^{L} \frac{\left|\sqrt{Q_{R_w}} h_{R_w v_{k_i}} \sqrt{Q_{v'_{k_j}}} h_{v'_{k_j} R_w} y_{v'_{k_j}}\right|^2}{\left|\sqrt{Q_{R_w}} h_{R_w v_{k_i}} \sigma^2_{R_w}\right|^2}. \tag{51}$$

Hence, we square both sides of (70) and have

$$\frac{(\varphi_1(R_{g*}))^2}{(\varphi_2(R_{g*}))^2} \geq \frac{(\varphi_1(R_{g*}) + \sum_{p=1}^{N-1} \varphi_1(R'_p))^2}{(\varphi_2(R_{g*}) + \sum_{p=1}^{N-1} \varphi_2(R'_p))^2}. \tag{71}$$

With the help of conclusions for $L = 2$, we have

$$\frac{(\varphi_1(R_{g*}))^2}{(\varphi_2(R_{g*}))^2} \geq \frac{(\varphi_1(R_{g*}) + \sum_{p=1}^{N-1} \varphi_1(R'_p))^2}{(\varphi_2(R_{g*}) + \sum_{p=1}^{N-1} \varphi_2(R'_p))^2} \geq \frac{0}{(\sigma^2_{v_{k_i}})^2}. \tag{72}$$

Therefore if $L = N$, the upper bound is given by (73), where:

$$SNR_{v'_{k_j}\to v_{k_i}}^{\{R_L\}} = \frac{(\varphi_1(R_{g*}) + \sum_{p=1}^{N-1} \varphi_1(R'_p))^2}{(\varphi_2(R_{g*}) + \sum_{p=1}^{N-1} \varphi_2(R'_p))^2 + (N\sigma^2_{v_{k_i}})^2}. \tag{74}$$

On the other hand, since $\sigma^2_{R'_1} \to 0^+, \sigma^2_{R'_2} \to 0^+, ..., \sigma^2_{R'_{L_0}} \to 0^+$, for $(R'_1, R'_2, ..., R'_{L_0})$, we assume that

$$\varphi_2(R'_1) \to 0^+, \varphi_2(R'_2) \to 0^+, ..., \varphi_2(R'_{L_0}) \to 0^+, \tag{75}$$

Since the noise appears at the receiver, if we select these relays, corresponding SNR can be derived as:

$$\frac{(\varphi_1(R_{g*}) + \sum_{g=1}^{L_0} \varphi_1(R_g))^2}{(\varphi_2(R_{g*}))^2 + (\sigma^2_{v_{k_i}} + L_0\sigma^2_{v_{k_i}})^2}. \tag{76}$$

In a special case, if we extract relative main signals for different cooperative paths and eliminate noise at the receiver v_{k_i}, the upper bound of SNR is given by

$$\frac{(\varphi_1(R_{g*}) + \sum_{g=1}^{L_0} \varphi_1(R_g))^2}{(\varphi_2(R_{g*}))^2 + (\sigma^2_{v_{k_i}})^2}. \tag{77}$$

APPENDIX C
PROOF OF LEMMA 3

The total SNR based on relays subset $\{R_L\}$ is expressed as:

$$\sum_{w=1}^{L} SNR_{v'_{k_j}\to v_{k_i}}^{R_w} \leq \max \sum_{w=1}^{L} SNR_{v'_{k_j}\to v_{k_i}}^{R_w}. \tag{78}$$

In (79), for relays subset $\{R_L\}$, different relays correspond to different power, fading coefficients, noise power, etc. So $\forall R_w \in \{R_L\}$, we define different sequences as

$$\begin{cases} A_w = \sqrt{Q_{v'_{k_j}}} h_{v'_{k_j} R_w} y_{v'_{k_j}} \\ B_w = \sqrt{Q_{R_w}} h_{R_w v_{k_i}} \\ C_w = \sigma^2_{R_w}, \end{cases} \tag{80}$$

Therefore, the right-hand-side of (79) can be expressed as

$$\max \sum_{w=1}^{L} \frac{(A_w B_w)^2}{(B_w C_w)^2 + (\sigma^2_{v_{k_i}})^2}. \tag{81}$$

Next, we seek solution for the upper bound in (81). For A_w and C_w, we have:

$$\begin{cases} \sum_{w=1}^{L} SNR_{v'_{k_j}\to v_{k_i}}^{\{R_L\}} \propto A_w \\ \sum_{w=1}^{L} SNR_{v'_{k_j}\to v_{k_i}}^{\{R_L\}} \propto \frac{1}{C_w}. \end{cases} \tag{82}$$

By defining $A_w = \tilde{A}$ and $C_w = \tilde{C}$, so if $0 \leq B_w \leq B_{w+1}$, we have:

$$B_w^2 B_{w+1}^2 \tilde{C}^2 + B_w^2 \sigma^4_{v_{k_i}} \leq B_{w+1}^2 B_w^2 \tilde{C}^2 + B_{w+1}^2 \sigma^4_{v_{k_i}}. \tag{83}$$

Furthermore, we obtain:

$$\frac{\tilde{A}^2 B_w^2}{B_w^2 \tilde{C}^2 + \sigma^4_{v_{k_i}}} \leq \frac{\tilde{A}^2 B_{w+1}^2}{B_{w+1}^2 \tilde{C}^2 + \sigma^4_{v_{k_i}}}. \tag{84}$$

Hence, we have

$$\sum_{w=1}^{L} SNR_{v'_{k_j}\to v_{k_i}}^{\{R_L\}} \propto B_w. \tag{85}$$

Therefore, $\max \sum_{w=1}^{L} SNR_{v'_{k_j}\to v_{k_i}}^{\{R_L\}} \propto B_w$ is obtained as high as possible for $\max A_w$, $\max B_w$ and as low as possible for $\min C_w$.

REFERENCES

[1] W.-C. Chien, H.-H. Cho, C.-F. Lai, F.-H. Tseng, H.-C. Chao, M. M. Hassan, and A. Alelaiwi, "Intelligent architecture for mobile hetnet in B5G," *IEEE Network*, vol. 33, no. 3, pp. 34–41, 2019.

[2] H. Bagheri, M. Noor-A-Rahim, Z. Liu, H. Lee, D. Pesch, K. Moessner, and P. Xiao, "5G NR-V2X: Toward connected and cooperative autonomous driving," *IEEE Communications Standards Magazine*, vol. 5, no. 1, pp. 48–54, 2021.

[3] I. Tomkos, D. Klonidis, E. Pikasis, and S. Theodoridis, "Toward the 6G network era: Opportunities and challenges," *IT Professional*, vol. 22, no. 1, pp. 34–38, 2020.

[4] M. Noor-A-Rahim, Z. Liu, H. Lee, M. O. Khyam, J. He, D. Pesch, K. Moessner, W. Saad, and H. V. Poor, "6G for vehicle-to-everything (V2X) communications: Enabling technologies, challenges, and opportunities," *Proceedings of the IEEE*, vol. 110, no. 6, pp. 712–734, 2022.

[5] M. Giordani, M. Polese, M. Mezzavilla, S. Rangan, and M. Zorzi, "Toward 6G networks: Use cases and technologies," *IEEE Communications Magazine*, vol. 58, no. 3, pp. 55–61, 2020.

$$\frac{(\varphi_1(R_{g*}))^2}{(\varphi_2(R_{g*}))^2+(\sigma^2_{v_{k_i}})^2} \geq \frac{(\varphi_1(R_{g*})+\sum_{p=1}^{N-1}\varphi_1(R'_p))^2}{(\varphi_2(R_{g*})+\sum_{p=1}^{N-1}\varphi_2(R'_p))^2+(\sigma^2_{v_{k_i}})^2} \geq \frac{(\varphi_1(R_{g*})+\sum_{p=1}^{N-1}\varphi_1(R'_p))^2}{(\varphi_2(R_{g*})+\sum_{p=1}^{N-1}\varphi_2(R'_p))^2+(N\sigma^2_{v_{k_i}})^2}. \quad (73)$$

$$\sum_{w=1}^{L} SNR^{R_w}_{v'_{k_j}\to v_{k_i}} \leq \max \sum_{w=1}^{L} \frac{(\sqrt{Q_{R_w}}h_{R_w v_{k_i}}\sqrt{Q_{v'_{k_j}}}h_{v'_{k_j}R_w}y_{v'_{k_j}})^2}{(\sqrt{Q_{R_w}}h_{R_w v_{k_i}}\sigma^2_{R_w})^2+(\sigma^2_{v_{k_i}})^2}. \quad (79)$$

[6] D. C. Nguyen, M. Ding, P. N. Pathirana, A. Seneviratne, J. Li, D. Niyato, O. Dobre, and H. V. Poor, "6G internet of things: A comprehensive survey," *IEEE Internet of Things Journal* , vol. 9, no. 1, pp. 359–383, 2022.

[7] N.-N. Dao, Q.-V. Pham, N. H. Tu, T. T. Thanh, V. N. Q. Bao, D. S. Lakew, and S. Cho, "Survey on aerial radio access networks: Toward a comprehensive 6G access infrastructure," *IEEE Communications Surveys Tutorials*, vol. 23, no. 2, pp. 1193–1225, 2021.

[8] F. Tang, Y. Kawamoto, N. Kato, and J. Liu, "Future intelligent and secure vehicular network toward 6G: Machine-learning approaches," *Proceedings of the IEEE* , vol. 108, no. 2, pp. 292–307, 2020.

[9] J. He, K. Yang, and H.-H. Chen, "6G cellular networks and connected autonomous vehicles," *IEEE Network*, vol. 35, no. 4, pp. 255–261, 2021.

[10] Y. Hui, N. Cheng, Y. Huang, R. Chen, X. Xiao, C. Li, and G. Mao, "Personalized vehicular edge computing in 6G," *IEEE Network*, vol. 35, no. 6, pp. 278-284, 2021.

[11] F. Liu, G. Tang, Y. Li, Z. Cai, X. Zhang, and T. Zhou, "A survey on edge computing systems and tools," *Proceedings of the IEEE*, vol. 107, no. 8, pp. 1537–1562, 2019.

[12] P. Arthurs, L. Gillam, P. Krause, N. Wang, K. Halder, and A. Mouzakitis, "A taxonomy and survey of edge cloud computing for intelligent transportation systems and connected vehicles," *IEEE Transactions on Intelligent Transportation Systems*, vol. 23, no. 7, pp. 6206-6221, 2021.

[13] R. Bruschi, F. Davoli, P. Lago, and J. F. Pajo, "A multi-clustering approach to scale distributed tenant networks for mobile edge computing," *IEEE Journal on Selected Areas in Communications*, vol. 37, no. 3, pp. 499–514, 2019.

[14] D. Wu, L. Zhou, Y. Cai, and Y. Qian, "Collaborative caching and matching for D2D content sharing," *IEEE Wireless Communications*, vol. 25, no. 3, pp. 43–49, 2018.

[15] M. Merluzzi, P. D. Lorenzo, S. Barbarossa, and V. Frascolla, "Dynamic computation offloading in multi-access edge computing via ultra-reliable and low-latency communications," *IEEE Transactions on Signal and Information Processing over Networks*, vol. 6, pp. 342–356, 2020.

[16] C. She, Y. Duan, G. Zhao, T. Q. S. Quek, Y. Li, and B. Vucetic, "Crosslayer design for mission-critical IoT in mobile edge computing systems," *IEEE Internet of Things Journal* , vol. 6, no. 6, pp. 9360–9374, 2019.

[17] M. Cosovic, A. Tsitsimelis, D. Vukobratovic, J. Matamoros, and C. Anton-Haro, "5G mobile cellular networks: Enabling distributed state estimation for smart grids," *IEEE Communications Magazine*, vol. 55, no. 10, pp. 62–69, 2017.

[18] Q.-V. Pham, H. T. Nguyen, Z. Han, and W.-J. Hwang, "Coalitional games for computation offloading in NOMA-enabled multi-access edge computing," *IEEE Transactions on Vehicular Technology*, vol. 69, no. 2, pp. 1982–1993, 2020.

[19] H. Huang, S. Hu, T. Yang, and C. Yuan, "Full-duplex non-orthogonal multiple access with layers-based optimized mobile relays subsets algorithm in B5G/6G ubiquitous networks," *IEEE Internet of Things Journal* , vol. 8, no. 20, pp. 15081–15095, 2021.

[20] K. Lin, Y. Li, Q. Zhang, and G. Fortino, "AI-driven collaborative resource allocation for task execution in 6G-enabled massive IoT," *IEEE Internet of Things Journal*, vol. 8, no. 7, pp. 5264–5273, 2021.

[21] P. Georgakopoulos, T. Akhtar, I. Politis, C. Tselios, E. Markakis, and S. Kotsopoulos, "Coordination multipoint enabled small cells for coalition-game-based radio resource management," *IEEE Network*, vol. 33, no. 4, pp. 63–69, 2019.

[22] W. Qi, Q. Li, Q. Song, L. Guo, and A. Jamalipour, "Extensive edge intelligence for future vehicular networks in 6G," *IEEE Wireless Communications*, vol. 28, no. 4, pp. 128–135, 2021.

[23] Y. Zhou, C. Pan, P. L. Yeoh, K. Wang, M. Elkashlan, B. Vucetic, and Y. Li, "Secure communications for UAV-enabled mobile edge computing systems," *IEEE Transactions on Communications*, vol. 68, no. 1, pp. 376–388, 2020.

[24] B. Yang, X. Cao, K. Xiong, C. Yuen, Y. L. Guan, S. Leng, L. Qian, and Z. Han, "Edge intelligence for autonomous driving in 6G wireless system: Design challenges and solutions," *IEEE Wireless Communications*, vol. 28, no. 2, pp. 40–47, 2021.

[25] H. Xiao, Y. Hu, K. Yan, and S. Ouyang, "Power allocation and relay selection for multisource multirelay cooperative vehicular networks," *IEEE Transactions on Intelligent Transportation Systems*, vol. 17, no. 11, pp. 3297–3305, 2016.

[26] L. Liu, C. Hua, C. Chen, and X. Guan, "Semidistributed relay selection and power allocation for outage minimization in cooperative relaying networks," *IEEE Transactions on Vehicular Technology*, vol. 66, no. 1, pp. 295–305, 2017.

[27] R. S. Thoma, C. Andrich, G. D. Galdo, M. Dobereiner, M. A. Hein, M. Kaske, G. Schafer, S. Schieler, C. Schneider, A. Schwind, and P. Wendland, "Cooperative passive coherent location: A promising 5G service to support road safety," *IEEE Communications Magazine*, vol. 57, no. 9, pp. 86–92, 2019.

He Huang received his Ph.D degree in school of Information and Communication Engineering, Beijing University of Posts and Telecommunications of China (BUPT), and he is now assistant professor with Chengdu University of Information and Technology of China (CUIT). He serves as reviewers for several journals, such as, IEEE Transactions on wireless communications, IEEE Transactions on Communications, IEEE Access, IEEE Communication letters, International Journal of Electronics and Physical Communications, and for IEEE Conference WCNC. His main research interests include critical technologies in 6G, industrial IoT, edge computing and so on.

Zilong LIU (Senior Member, IEEE) received the bachelor's degree from the School of Electronics and Information Engineering, Huazhong University of Science and Technology (HUST), China, in 2004, the master's degree from the Department of Electronic Engineering, Tsinghua University, China, in 2007, advised by Prof. Huazhong Yang (an IEEE Fellow), and the Ph.D. degree from the School of Electrical and Electronic Engineering, Nanyang Technological University (NTU), Singapore, in 2014, advised by Prof. Yong Liang Guan. His Ph.D. thesis "Perfect- and Quasi- Complementary Sequences," with a focus on fundamental limits, algebraic constructions, and the applications of complementary sequences in wireless communications, has settled a few long-standing open problems in the field. He was a Visiting Ph.D. Student with The Hong Kong University of Science and Technology (HKUST) hosted by Prof. Wai Ho Mow and the University of Melbourne hosted by Prof. Udaya Parampalli. From January 2018 to November 2019, he was a Senior Research Fellow at the Institute for Communication Systems (ICS), Home of the 5G Innovation Centre (5GIC), University of Surrey, during which he studied the air-interface design of 5G communication networks. Prior to his career in U.K., he spent nine and a half years at NTU, first as a Research Associate from July 2008 to October 2014 and then as a Research Fellow from November 2014 to December 2017. He was a Red Bird Visiting Scholar with HKUST from December 2023 to January 2024. He is currently an Associate Professor and the 6G Laboratory Manager of the School of Computer Science and Electronic Engineering, University of Essex. He has widely published in top-rated journals, such as IEEE TRANSACTIONS ON INFORMATION THEORY, IEEE TRANSACTIONS ON SIGNAL PROCESSING, and PROCEEDINGS OF THE IEEE. So far, he has made a series of original contributions to sequences, waveforms, and multiple access. His research interests include the interplay of coding, signal processing, and communications, with a major objective of bridging theory and practice. His recent research interests include new waveforms for 6G and beyond, the synergies between communication, sensing, and localization, as well as machine learning for enhanced communications and networking. He was a Committee Member of major IEEE conferences (e.g., ISIT'2026, PIMRC'2026, VTC-Fall'2025, IWSDA'2025, and PIMRC'2023). He was also an awardee of the prestigious New Investigator Award from the Engineering and Physical Sciences Research Council (EPSRC), U.K., in June 2023. He was named the 2024 Outstanding Mid-Career Researcher in the Faculty of Science and Health, University of Essex. He was the Hosting General Chair of the 12th Sequences and Their Applications (SETA'2024, https://seta-2024.github.io/) and the 10th IEEE International Workshop on Signal Design and Its Applications in Communications (iwsda2022.github.io). He is/was an Associate Editor of IEEE TRANSACTIONS ON WIRELESS COMMUNICATIONS, IEEE TRANSACTIONS ON VEHICULAR TECHNOLOGY, IEEE TRANSACTIONS ON NEURAL NETWORKS AND LEARNING SYSTEMS from April 2022 to July 2025, IEEE WIRELESS COMMUNICATIONS LETTERS, IEEE OPEN JOURNAL OF THE COMMUNICATION SOCIETY, and Advances in Mathematics of Communications. He was a Consultant of Japanese Government on 6G-assisted autonomous driving in January 2023. Details of his research can be found at: https://sites.google.com/site/zilongliu2357

Haishi Wang received his BS in Microelectronics from Sichuan University in 2004, and PhD in Microelectronics and Solid-state Electronics from University of Electronic Science and Technology of China in 2013. He is currently a Professor in the College of Communication Engineering and Microelectronics, Chengdu University of Information Technology. His current research interests include semiconductor devices, circuits and systems design. He is a specially appointed expert of Chengdu City and a reserve candidate for academic and technological leaders of Sichuan Province.

Wei Huang received the B.S. and M.S. degrees from Anhui University of Science and Technology, Huainan, China, in 2010 and 2013, respectively, and the Ph.D. degree in information and communication engineering from the School of Information Science and Engineering, Southeast University, Nanjing, China,in 2018. Since December 2018, he has been with the School of Computer Science and Information Engineering, Hefei University of Technology, where he is currently an Associate Professor. His research interests include B5G/6G wireless communications and intelligent signal processing. He has authored or co-authored more than 50 technical publications and held 20 invention patents granted. He was a recipient of the Natural Science Award from the Anhui Provincial Institute of Communications and the Best Paper Award at the IEEE ICC (Workshop) in 2024. He served as the Guest Editor for Sensors and a reviewer for various journals.

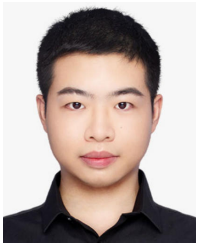

Chaojie Gu received the B.Eng. degree in information security from Harbin Institute of Technology, Weihai, China, in 2016, and the Ph.D. degree in computer science and engineering from Nanyang Technological University, Singapore, in 2020. In 2021, he was a Research Fellow with the Singtel Cognitive and Artificial Intelligence Laboratory for Enterprise. He is currently an Assistant Professor with the College of Control Science and Engineering, Zhejiang University, Hangzhou, China. His research interests include the IoT, industrial IoT, edge computing, and low-power wide area networks.

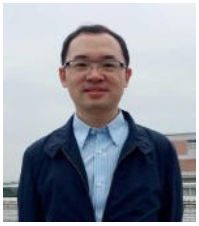

Zhiheng Hu received his Ph. D degreeh of Electronic Engineering from the University of Electronic Science and Technology of China (UESTC) in 2003. He is an associate professor in the College of Communication Engineering (College of Microelectronics), Chengdu University of Information Technology in China. His main research interests cover key technologies and engineering applications of wireless communication, mobile communication networks and services, intelligent information processing, adaptive signal processing.

Md. Noor-A-Rahim received the Ph.D. degree from the School of Information Technology and Mathematical Sciences, University of South Australia, Australia, in 2015. He is currently serving as an Assistant Professor (Lecturer-Above the Bar) with the School of Computer Science and Information Technology, University College Cork, Ireland, where he was a Senior Researcher and a Marie Curie Fellow. He also held the position of Postdoctoral Research Fellow with Nanyang Technological University, Singapore. His research interests include control over wireless networks, intelligent transportation systems, machine learning, signal processing, and DNA-based data storage. In recognition of his academic excellence, he was honored with the Michael Miller Medal for presenting the most outstanding Ph.D. thesis in 2015. For more information, see https://narahim.github.io/.